NANO LETTERS

2002
Vol. 2, No. 3
207−210

Irradiation of Dye-Doped Microspheres with a Strongly Focused Laser Beam Results in Alignment upon Optical Trapping

Garth J. Simpson,† Thorsten Wohland, and Richard N. Zare*

Department of Chemistry, Stanford University, Stanford California 94305-5080

Received September 20, 2001; Revised Manuscript Received December 12, 2001

ABSTRACT

The irradiation of dye-doped polystyrene microspheres with an argon ion laser (488 nm) changes their properties and creates photopatterns. These photopatterns can be manipulated by altering the location of the focal point inside the spheres. The illuminated microspheres subsequently undergo one-dimensional rotational diffusion about the optical axis when captured in an optical trap (985 nm). This behavior is well described by a model in which the differently irradiated portions of the microsphere possess different refractive indices.

1. Introduction. Micron-scale polymer particles are employed in numerous applications ranging from force measurements by optical tweezers to fluorescence assays in biology. These particles can be prepared with a wide range of surface functionality and/or charge, can be doped with a host of different fluorophores, and are often biocompatible.[1,2] We have recently demonstrated that controlled positioning of nanoscopic particles in radio frequency AC electric fields can lead to rotation of particle pairs. These rotating particles were assembled into microscopic "anti-gears", and have potential applications for microfluidic mixing, chemical/biological sensing, and incorporation into microelectromechanical devices.[3] The most readily available nano- and microscale polymer particles are spherical in shape; a condition that can mask an array of interesting phenomena. For example, it is difficult to measure rotational motions of spherical, homogeneous particles, as the physical and optical properties typically do not change with angle. Although intriguing schemes have been developed to overcome such obstacles,[4,5] complications associated with rotational measurements of spherical particles persist. In this letter, partial photobleaching of fluorescent polymer microspheres is demonstrated as a viable means both to photopattern the fluorescence profiles within spheres and to selectively align spherical particles about specific internal axes.

The forces that lead to trapping of a microscopic particle, which is much smaller than the laser wavelength, can be separated phenomenologically into a repulsive contribution from scatter F_{scatter}, which is proportional to the local intensity, and an attractive contribution F_{grad}, which is proportional to the local intensity gradient.[6] For an inhomogeneous particle that is larger than the wavelength of the trapping beam, the potential energy will generally also depend on particle orientation within the trap. Mathematically, the potential energy V for a given particle position and orientation can be evaluated by summing together the energy required to position each infinitesimal volume element into a given three-dimensional configuration.

In this letter, we demonstrate that preferred alignment can be induced in spherical microscopic particles following treatment by laser irradiation. Photobleaching or photoalteration can destroy the symmetry of a particle. In turn, the particle can orient to minimize its potential energy. In the Supporting Information we give qualitative calculations that are derived from equations for gradient and scattering forces in the Rayleigh limit (i.e., for particle radii r much smaller than the laser wavelength λ).

2. Experimental. Fluorescent microspheres were purchased from Molecular Probes (2 μm and 4 μm diameter, polystyrene matrix) and Polysciences (3 μm diameter, calibration grade, latex matrix) and diluted in purified water prior to use. A telescoped beam from a 985 nm MOPA diode laser (300 mW, SDL model SDL-5762-A6) focused through a 100× oil immersion objective (Nikon, 1.4 N. A.) was used to trap the microspheres in the visible focal plane. Photobleaching was accomplished using focused 488 nm light from an argon ion laser (SpectraPhysics Stabilite 2017). Unless otherwise stated, the photobleach excitation duration was between 0.2 and 0.5 s, which was much less than the

* To whom correspondence should be addressed. E-mail: zare@stanford.edu.

† Present address: Department of Chemistry, Purdue University, West Lafayette, IN 47907.

10.1021/nl015632d CCC: $22.00
Published on Web 01/09/2002

rotational diffusion time for micron scale particles in water. Following photobleaching, wide-field laser induced fluorescence (LIF) images were acquired by attenuating the incident beam and passing it through a spinning disk diffuser, then imaging the emitted fluorescence through a dichroic mirror onto an silicon intensified target (SIT) camera (Hamamatsu C2400−08). The images were recorded onto video, subsequently imported into ScionImage (ScionCorp, Frederick, MD), and analyzed. The location of the optical trap within the focal plane was manipulated independently of the photobleach laser focal point by adjustment of a mirror and the telescope. Photobleaching out of the plane was accomplished by lowering the visible focal plane to just outside the coverslip.

Theoretical photobleach profiles were calculated assuming complete bleaching of all fluorophores directly illuminated by the excitation beam and no bleaching for fluorophores outside the beam. Effects related to reflection and polarization of the excitation beam within the sphere could be neglected in the reported calculations, as they essentially influence the internal light intensity, which is always assumed sufficient for complete photobleaching. For a sphere positioned such that the sphere center and the photoexcitation focal point are coincident, every incident ray enters normal to the sphere surface and refraction can be neglected. In excitation geometries off-center, refraction yields slight change in the direction of ray propagation through the spheres, but the refractive index difference between water and latex is sufficiently small that these effects only yield subtle changes in the ray propagation directions and in the resulting bleach patterns. To simplify calculations, these refraction effects were not included. The theoretical profiles were generated by integrating over the remaining unbleached three-dimensional fluorescence pattern for a given orientation within the object plane.

Calculations of the potential energy surfaces (i.e., potential energy as a function of photobleach location and sphere orientation) were performed for a particle diameter of 3 μm by combining the theoretical photobleach profiles with the intensity distribution expected for a focused 300 mW Gaussian beam.[7] Photobleached portions of the sphere were arbitrarily assigned a refractive index of 1.60, compared with a refractive index of 1.59 in the unbleached portions (both values within the range typical for polystyrene). Use of different refractive indices yielded qualitatively similar potential energy surfaces, provided the refractive index within the bleached portions was greater than within the unbleached portions. Following Wohland et al.,[8] calculations were performed for a sphere positioned radially at the center of the trap beam, and displaced axially from the trap laser focal point along the direction of propagation by a distance equal to the particle radius.

Rotational diffusion measurements were made on 2 μm diameter spheres following photobleaching under two conditions; one set for rapid photobleaching at high intensities (~40 mW of focused 488 nm excitation) and another set for lower intensities (~10−20 mW). Diffusion parameters were determined by evaluating the distance and angle between the geometric sphere center and the center of fluorescence intensity at each time step in a series of 500 consecutive images separated by 0.1 s. Reported diffusion constants are the average values measured for time separations between 0.1 and 10 s.

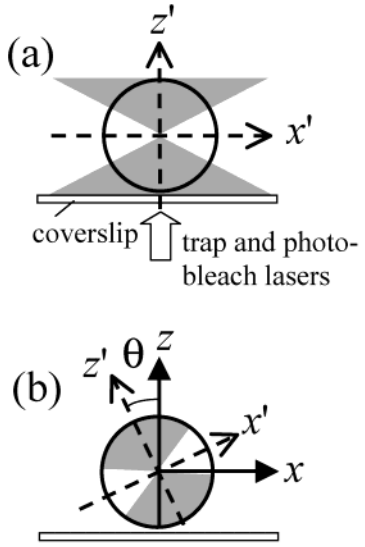

Figure 1. Experimental geometry and definition of coordinates: (a) the internal x'- and z'-axes of the sphere are defined with respect to the photoexcitation beam, and (b) following reorientation after photobleaching, the angle between the z'-axis and the z-axis (parallel to the propagation direction of both the photobleach and trap beams) is given by θ.

3. Results and Discussion. A phenomenological model was developed to treat optical trapping of partially photobleached spheres, in which photoexcitation resulted in an effective change in the refractive index within the photobleached regions of a fluorescent sphere (indicated by the darkened portions in Figure 1). It is not clear whether the change of refractive index is caused by the destruction of the fluorophores or by a change in the polymer properties or by the action of both mechanisms. Whatever the case, experiments indicate that long repeated irradiation under the same conditions induces visually detectable damage to the spheres (data not shown) and thus favors photoalteration of the polymer as the major explanation for this effect. Using the coordinates as defined in Figure 1, an optically trapped sphere was assumed to be photobleached with the excitation beam focused on a particular location within a sphere of radius r, thereby defining a set of internal axes, x', y', and z'. If the particle rotated after photoexcitation (e.g., by an angle θ as shown), the internal axes no longer necessarily coincided with the laboratory axes, x, y, and z (Figure 1b).

Theoretical potential energy curves, shown in Figure 2, were generated by performing numerical integration using this phenomenological approach for an increase in effective refractive index within the bleached portions of a sphere. The potential energy surfaces are shown as functions of both the polar tilt angle of the sphere z'-axis, θ, and the relative distance of the photobleach focal point from the sphere center. The curves at $x'/r = 0$ and $z'/r = 0$ are identical. Calculations performed for an effective decrease in refractive index within illuminated regions (not shown) yielded op-

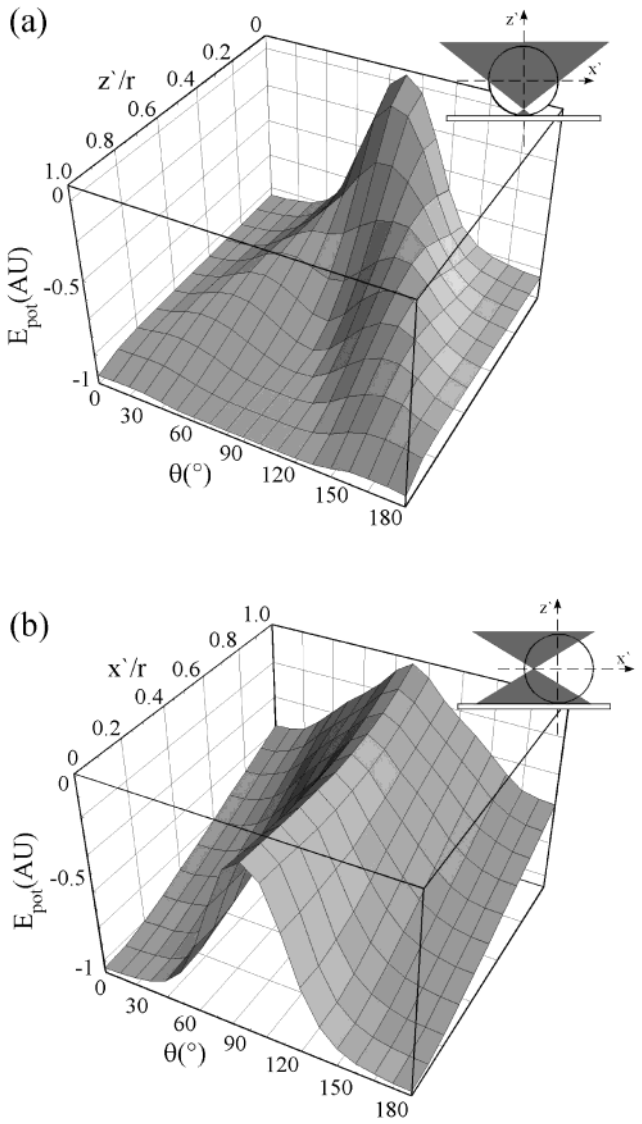

Figure 2. Potential energy curves for rotation in θ following irradiation with the excitation beam focus located (a) along the z'-axis and (b) along the x'-axis (for a twist angle of zero about z'). The potential energy has been normalized. The difference in refractive index between irradiated and nonirradiated parts of the particle has been 0.01. The values for $x'/r = z'/r = 0$ are identical for graphs (a) and (b). Note that in (a) a potential minimum grows in at $\theta = 90°$ for $z'/r > 0.5$.

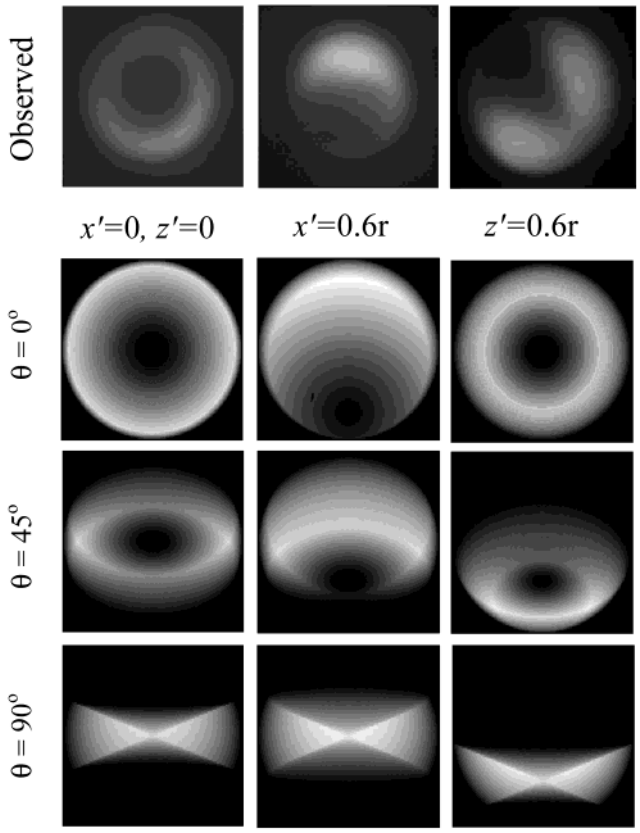

Figure 3. Experimental and theoretical LIF patterns for partially photobleached fluorescent spheres. The top row contains experimentally measured fluorescence images of 3 μm diameter spheres. They were acquired with the photobleach laser focused at $x' = 0$, $z' = 0$ (top left), at $r/2 < x' < r$, $z' = 0$ (top center), and at $x' = 0$, $r/2 < z' < r$ (top right). The bottom three rows contain the corresponding theoretical LIF profiles evaluated for different tilt angles θ, indicated to the left. By inspection, the experimentally measured fluorescence profile for bleaching at the sphere center (left column) corresponds to an alignment axis of approximately 0° (i.e., the sphere is aligned along the original the photoexcitation internal axis). A similar preferred orientation was observed for photoexcitation focused off-center but within the object plane (center column), but an out-of-plane excitation focus yielded an experimental profile more consistent with higher orientation angles (between ~45° to 90°).

posite trends (i.e., potential energy minima and maxima were inverted). Although Rayleigh-limited expressions for the forces within an optical trap are only quantitatively reliable for particles much smaller than the wavelength of light, these equations can still be used to probe qualitative trends (see supplement).

Figure 3 presents a comparison between the experimentally measured LIF profiles and theoretical fluorescence profiles. The experimentally measured images shown in the top row of Figure 3 were acquired with the bleaching laser beam focused in the center of the sphere (top left), along the x'-axis but near the sphere edge (top center), and along the z'-axis of the sphere but near the edge (top right). The theoretical profiles were generated by integration of the fluorescence intensity distribution normal to the focal plane (i.e., along the laboratory z-axis), as if viewed from above for a given location of the excitation focal point within the sphere.[9] For each of the three excitation focal points considered, theoretical profiles were evaluated for three different polar orientation angles of the sphere z'-axis (i.e., for a given tilt angle of the sphere following photobleaching). Although the trapped spheres were observed to rotate within the focal plane following photobleaching, the general shape of the LIF patterns shown did not change significantly over time (i.e., out-of-plane rotational diffusion was not observed).

The experimental time-dependent fluorescence images were analyzed to yield rotational diffusion constants and the normalized variance in the distance d between the geometric sphere center and the center of fluorescence, given by $(\langle d^2\rangle - \langle d\rangle^2)/\langle d\rangle^2$. The parameter $(\langle d^2\rangle - \langle d\rangle^2)/\langle d\rangle^2$ is a qualitative indicator for three-dimensional vs one-dimensional rotational diffusion. If the particle rotates only within the object plane,

the distance d should be nearly constant, yielding a normalized variance approaching 0. If there is out of plane rotation, the normalized variance will differ from 0.

By controlling the photobleach excitation intensity and/or duration or alternatively by reducing or increasing the intensity of the trap laser, partially photobleached spheres could be prepared with or without perceptible alignment. Photobleaching under mild excitation conditions did not lead to a preference in orientation, indicating that the illumination process induced the alignment. A partially photobleached sphere immobilized in a weak trap yielded $(\langle d^2\rangle - \langle d\rangle^2)/\langle d\rangle^2 = 0.24 \pm 0.05$, whereas the same sphere yielded $(\langle d^2\rangle - \langle d\rangle^2)/\langle d\rangle^2 = 0.04 \pm 0.03$ upon increasing the trap power and inducing alignment (3 measurements at each power, 500 images per measurement). Consistent with empirical observations, the smaller variance in d observed in aligned spheres suggests an essentially constant fluorescence profile changing in time only in the rotational angle within the focal plane. A one-dimensional diffusion coefficient of $0.18\ s^{-1} \pm 0.06\ s^{-1}$ ($N = 6$) was obtained for aligned and trapped 2 μm diameter spheres, compared with an expected diffusion constant[10] in water of $0.185\ s^{-1}$.

Inspection of Figures 2 and 3 reveals evidence supporting the proposed model, in which photobleached portions of the sphere exhibit an effective increase in relative refractive index. The spheres bleached with the excitation beam focused near the sphere center produced ring-like patterns in wide-field fluorescence measurements, consistent with the theoretical LIF pattern calculated for alignment along the z'-axis, and a preferred orientation angle of $\theta \cong 0°$. For spheres bleached within the focal plane but off-center (i.e., along the x'-axis, center column of Figure 3), the theoretical and experimental fluorescence images also support axial alignment and low orientation angles, θ. In contrast, the experimental LIF profiles for spheres bleached along the z'-axis near the sphere edge are most consistent with the theoretical profile for $\theta \cong 90°$. The apparent mismatch in the internal angle in the photobleach profiles likely results from use of an excitation beam with a spatial profile that did not fill the back of the microscope objective, resulting in an effective numerical aperture less than the theoretical maximum. Spheres bleached along the z'-axis appear to exhibit a bimodal behavior, adopting axial alignment for an excitation focal point located near the sphere center (e.g., left column in Figure 3), but the LIF patterns acquired for excitation focused near the sphere edge are more consistent with $\theta \cong 90°$ and the z'-axis lying within the focal plane (right column in Figure 3). All three of the experimental fluorescence profiles and trends in orientation are in excellent agreement with the angles of the energy minima in the calculated potential energy curves shown in Figure 2. We have shown that our calculations, although not quantitative, predict the forces and trapping positions of an optical trap qualitatively. Rigorous theoretical treatments of optical trapping forces can be found in Sheetz[11] and Rohrbach and Stelzer[12] and references therein.

To summarize, we have developed a methodology to photoinduce unique alignment axes within optically trapped fluorescent microspheres and to create optically detectable patterns to measure their alignment and rotation. The experiments show excellent qualitative correspondence with theoretical predictions based on a simple model that assumes Rayleigh scattering and that the photoalteration of the polymer can be represented by a change in the refractive index of the polymer. Induced alignment in beads could be particularly advantageous in force measurements by optical tweezers to limit unwanted torque on the measurement system from rotational diffusion. Other applications of this method include in situ flow measurements in liquids, e.g., on microchips, by measurement of bead rotation or the mapping of microscale viscosity from localized rotational diffusion measurements. Optical tweezers have been used for surface imaging.[13] With alignment of beads this method can be extended to measure friction by monitoring the orientation of a bead while it is dragged over a surface. Therefore the alignment of beads open up new applications from microchip technology to biophysical measurements.

Acknowledgment. The authors would like to acknowledge funding from the National Institute on Drug Abuse and from Pfizer and the Life Sciences Research Foundation. T.W. acknowledges funding from the Swiss National Science Foundation.

Supporting Information Available: Estimation of orientation of particles in an optical trap. Qualitative calculations are derived from equations for gradient and scattering forces in the Rayleigh limit. This material is available free of charge via the Internet at http://pubs.acs.org.

References

(1) Kawaguchi, H. *Prog. Polym. Sci.* **2000**, *25*, 1171.
(2) Arshady, R. *Biomaterials* **1993**, *14*, 5.
(3) Simpson, G.; Wilson, C. F.; Gericke, K.-H.; Zare, R. N. *ChemPhysChem*, in press.
(4) Brody, J. P.; Quake, S. R. *Appl. Phys. Lett.* **1999**, *74*, 144.
(5) Barrall, G. A.; Schmidt-Rohr, K.; Lee, Y. K.; Landfester, K.; Zimmermann, H.; Chingas, G. C.; Pines, A. *J. Chem. Phys.* **1995**, *104*, 509.
(6) Block, S. M. *Noninvasive Techniques in Cell Biology*; Foskett, J. K., Grinstein, S., Eds.; Wiley and Sons: New York, 1990; Chapter 15.
(7) Saleh, B. E. A.; Teich, M. C. *Fundamentals of Photonics*; Wiley and Sons: New York, 1991, Chapter 3.
(8) Wohland, T.; Rosin, A.; Stelzer, E. H. K. *Optik* **1996**, *102*, 181.
(9) Boundary conditions for calculation of the fluorescence profiles were identical to those described in ref 6, assuming a fluorescence intensity of zero in the bleached regions and constant intensity per unbleached volume element.
(10) Berg, H. C. *Random Walks in Biology*; Princeton University Press: Princeton, 1983; Chapter 6.
(11) *Laser Tweezers in Cell Biology*; Sheetz, M., Ed.; Academic Press: San Diego, 1998.
(12) Rohrbach, A.; Stelzer, E. H. K. *J. Opt. Soc. Am. A* **2001**, *18*(4), 839.
(13) Florin, E.-L.; Pralle, A.; Hörber, J. K. H.; Stelzer, E. H. K. *J. Struct. Biol.* **1997**, *119*, 202−211.

NL015632D